A Study of the Mechanism of Hardness Change of Al-Zn-Mg Alloy during Retrogression Reaging Treatments by Small Angle X-ray Scattering (SAXS)

CHAOFU MENG, HOUWEN LONG, and YONG ZHENG

In this work, the changes in hardness of Al-Zn-Mg alloy during retrogression and reaging (RRA) treatments were detected and the mechanism of the hardness change was studied by Small Angle X-ray Scattering (SAXS). It was discovered that the hardness changes during RRA treatments are as follows. (1) Hardness decreases at the beginning of retrogression, achieves a minimum value at 90 seconds, and then increases and achieves the second maximum value at 6 minutes, and finally decreases simply. (2) Hardness of the reaged sample is higher than that of the retrogressed sample. The following conclusions were drawn from the experimental results of SAXS. (1) The drop in hardness for short retrogression time is attributed to the decrease of volume fraction of the precipitates and the growth of the particles; the drop in hardness with increasing retrogression time after the second maximum of hardness achieved is attributed to coarsening of the particles. 2. The increase in hardness during reaging is due to the occurrence of new precipitates and the increase of volume fraction of the precipitates.

I. INTRODUCTION

The Al-Zn-Mg alloys are susceptible to stress corrosion cracking (SCC). The degree of susceptibility depends on the aging condition and can be reduced by overaging, which leads to a sacrifice of the maximum strength. Recently, a new heat-treatment procedure called retrogression and reaging (RRA) was devised for 7000 system alloys by Cina.[1] This method produces a several-fold increase in the threshold stress for SCC over that of 7075-T6 without a sacrifice of maximum strength. The RRA treatment consists of a short time retrogression anneal applied to 7075-T6 in a temperature range within the two-phase field of the phase diagram, followed by water quenching and a final reaging treatment equivalent to the original T6 tempe.[1] Some authors studied the changes of microstructure during the retrogression and reaging in 7075 alloy by means of transmission electron microscopy (TEM), and some controversial views upon the nature of the benefits of the RRA treatment were proposed. Although some authors believed that the high strength of the 7075 alloy in reaged sample is considered to arise from the high overall concentration of the particle in this structure, no quantitative results have been obtained.[2–6]

A Small Angle X-ray Scattering (SAXS) study on the change of microstructure in Al-Zn-Mg alloy during RRA treatments has been performed. On the basis of previous work,[7] this article investigated the mechanism of hardness change during RRA treatment quantitatively by means of SAXS.

CHAOFU MENG, Professor, HOUWEN LONG, Associate Professor, and YONG ZHENG, Student, are with the Materials Science Institute, Jilin University, Changchun 130023, People's Republic of China.

Manuscript submitted April 30, 1996.

II. EXPERIMENTAL

The alloy composition is 1.5 wt pct Cu, 5.8 pct Zn, 2.4 pct Mg, 0.4 pct Mn, 0.5 pct Fe, 0.4 pct Si, and balance Al. The sizes of the sample were $35 \times 10 \times 0.08$ mm^3 for SAXS experiments and $20 \times 10 \times 1.5$ mm^3 for hardness measurement. The samples were polished mechanically on two surfaces with grits. The RRA treatment consists of three stages:

(1) heating at 470 °C for 40 minutes, followed by water quenching and aging at 120 °C for 24 hours;
(2) retrogression treatment at 200 °C for various periods, followed by water quenching; and
(3) reaging at 120 °C for 24 hours.

For the sample treated at each stage of the RRA treatments, SAXS intensity and Rockwell hardness with A scale were measured. The SAXS experiments were carried out on a *D*/max-*rA* diffractometer with a long-slits collimation system. The widths of the collimation slits are 0.04, 0.03, and 0.05 mm, respectively, while that of the detector slit is 0.1 mm. The Cu $K\alpha$ radiation with a Ni filter, a tube current of 180 mA, and a tube voltage of 55 kV was used. A step scan technique was used with a step width of 0.02 deg, accounting time of 20 seconds for each step, and a scanning range from 0.1 to 2 deg. The background intensity was subtracted.

III. RESULTS

To simplify the description, the following notation is used. The aged sample represents the sample heated at 470 °C for 40 minutes, followed by water quenching, and aged at 120 °C for 24 hours. The retrogressed sample represents the sample heated at 470 °C for 40 minutes, followed by water quenching, aged at 120 °C for 24 hours, and then retrogressed at 200 °C for various periods. The reaged sample represents the sample heated at 470 °C for 40 minutes, followed by water quenching, aged at 120 °C for 24 hours,

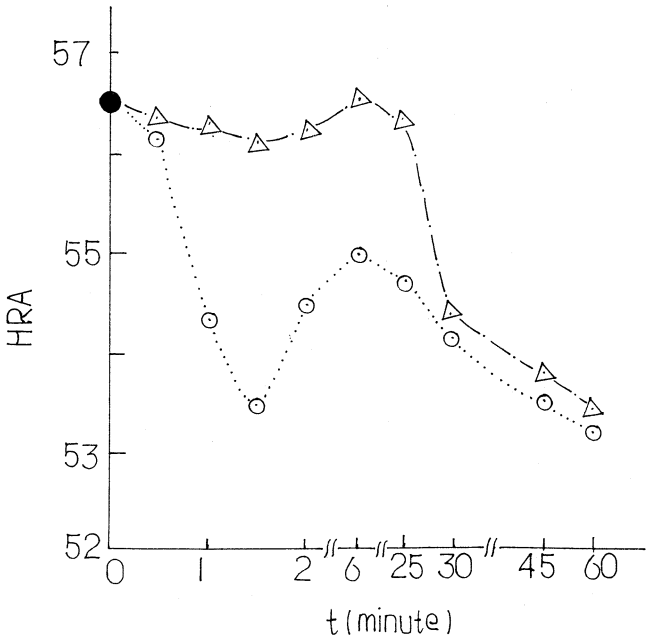

Fig. 1—Hardness (HRA)–retrogression time relationship curves. (●) for the aged sample, (◯) for the samples retrogression at 200 °C for various periods, and (△) for the samples retrogression at 200 °C for various periods and then reaged.

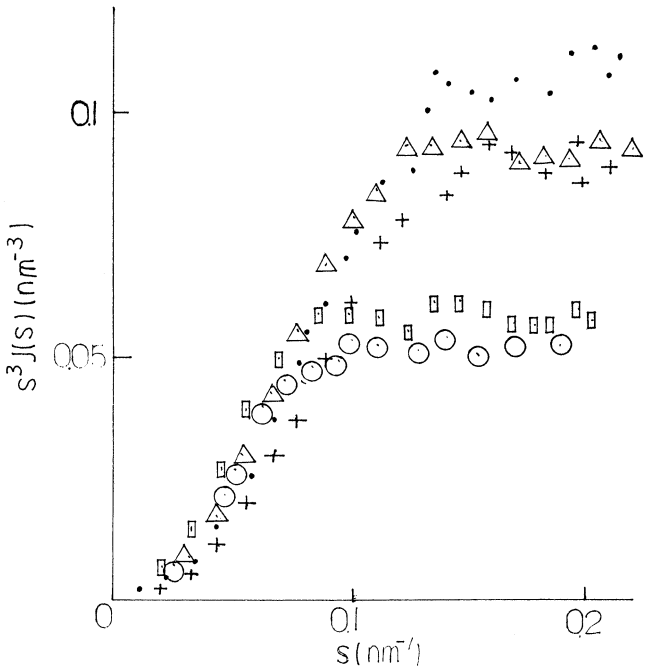

Fig. 3—s^3 (s)-s plots: (·) for sample 1, (+) for sample 2, (△) for sample 3, (◯) for sample 4, and (□) for sample 5.

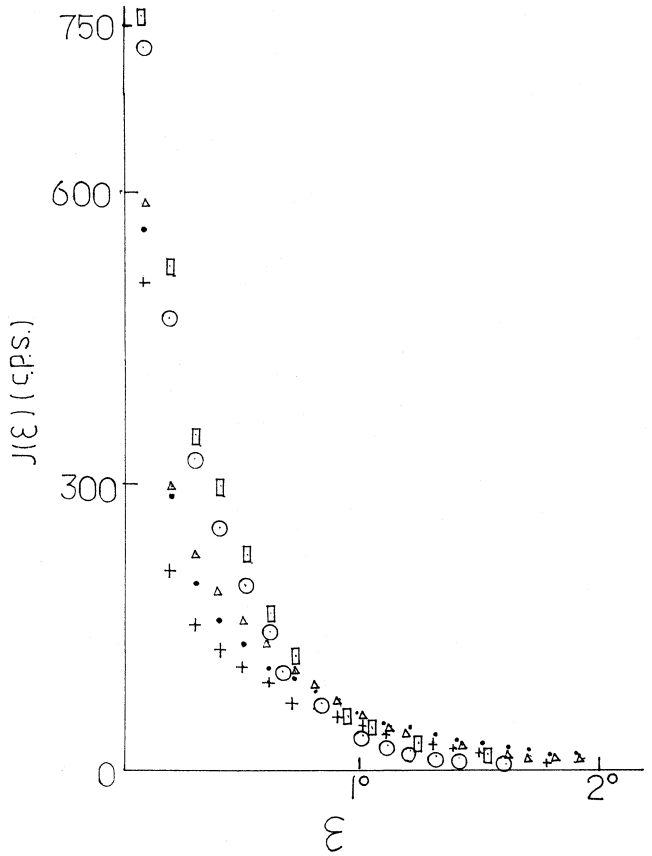

Fig. 2—$J(\varepsilon)$-ε curves: (·) for sample 1, (+) for sample 2, (△) for sample 3, (◯) for sample 4, and (□) for sample 5.

retrogressed at 200 °C for various periods, and finally reaged at 120 °C for 24 hours.

In Figure 1, the hardness curves are shown for the samples treated at each stage of RRA: (●) represents the hardness of the aged sample; (◯) represents the hardness of the samples retrogressed at 200 °C for various periods; and (△) represents the hardness of the reaged samples. One can see the following from Figure 1: (1) hardness of the retrogressed sample is lower than that of the aged sample and changes with retrogression time. It decreases at the beginning of the retrogression, achieves a minimum value at 90 seconds, increases and achieves the second maximum value at 6 minutes, and finally decreases simply. (2) Hardness of the reaged sample depends on retrogression time also. (3) Hardness of the reaged sample is higher than that of the retrogressed sample but is still lower than that of the aged sample, except the sample retrogressed at 200 °C for 6 minutes and then reaged; the latter has the same hardness as that of the aged sample.

In Figure 2, SAXS intensity curves are shown: (·) for sample 1, (+) for sample 2, (△) for sample 3, (◯) for sample 4, and (□) for sample 5.

In Figure 3, $s^3J(s)$-s curves are shown; here, $J(s)$ is the intensity obtained by using the long-slits collimation system, $s = 2\sin\theta/\lambda$, $\theta = \varepsilon/2$, ε is the scattering angle, and λ is the wavelength of X-rays. From Figure 3, it can be seen that $s^3J(s)$ approaches a constant K_p' at large value of s:

$$\lim_{s\to\infty} [s^3 J(s)] = K_p' \tag{1}$$

The constant K_p' is related to specific inner surfaces, S_p, by Eq. [2]:[7,8,9]

$$S_p = 8\pi K_p'/[I_e(\Delta\rho)^2 V] \tag{2}$$

where I_e is the scattering intensity of an electron, $\Delta\rho$ is the electron density difference between the particle and the ma-

Table I. The Values of K_P', $\tilde{Q}_S$, R_G, and HRA for the Samples Treated in Various Conditions*

Sample	Treating Conditions	K_P' (nm^{-3})	$\tilde{Q}_3$ (nm^{-2})	$\tilde{Q}_1 + \tilde{Q}_2$ (nm^{-2})	$\tilde{Q}_s$ (nm^{-2})	R_G (nm)	HRA
1	470 °C, 40 min quenching → 120 °C, 24 h aging	0.108 ± 0.002	0.68 ± 0.02	1.00 ± 0.02	1.68 ± 0.04	2.4 ± 0.1	56.5 ± 0.3
2	470 °C 40 min quenching → 120 °C 24 h aging + 200 °C 6 min retrogression	0.090 ± 0.002	0.57 ± 0.02	0.99 ± 0.02	1.56 ± 0.04	2.6 ± 0.1	55 ± 0.3
3	470 °C 40 min quenching → 120 °C 24 h aging + 200 °C 6 min retrogression + 120 °C, 24 h reaging	0.095 ± 0.002	0.60 ± 0.02	1.30 ± 0.02	1.90 ± 0.04	2.8 ± 0.1	56.5 ± 0.3
4	470 °C 40 min quenching → 120 °C 24 h aging + 200 °C 45 min retrogression	0.054 ± 0.002	0.34 ± 0.02	1.26 ± 0.02	1.60 ± 0.04	3.3 ± 0.1	53.5 ± 0.3
5	470 °C 40 min quenching → 120 °C 24 h aging + 200 °C 45 min retrogression + 120 °C, 24 h reaging	0.059 ± 0.002	0.37 ± 0.02	1.45 ± 0.02	1.82 ± 0.04	3.5 ± 0.1	53.8 ± 0.3
6	470 °C 40 min quenching → 120 °C 24 h aging + 200 °C 90 s retrogression	0.94 ± 0.002	0.62 ± 0.02	0.90 ± 0.02	1.52 ± 0.04	2.4 ± 0.1	53.5 ± 0.3
7	470 °C 40 min quenching → 120 °C 24 h aging + 200 °C 90 s retrogression 120 °C, 24 h reaging	0.104 ± 0.002	0.68 ± 0.02	1.16 ± 0.02	1.84 ± 0.04	2.5 ± 0.1	56.1 ± 0.3

*The values of K_P', $\tilde{Q}_S$, and R_G for samples 1 through 5 were obtained from Figs. 2 through 5.
In Figs. 2 through 5, the dates for samples 6 and 7 were not shown, to avoid the appearance of too many points of dates in the figures.
The values of K_p', $\tilde{Q}_S$, and R_G for samples 6 and 7 were obtained from figures similar to Figs. 2 through 5.

trix, V is the volume of sample irradiated by X-rays; I_e, $\Delta\rho$, and V are constant under unchanged experimental conditions. The values of K_p' are listed in Table I.

For an ideal two-phase system, $\tilde{Q}_s$ can be written as the following:[8,10]

$$\tilde{Q}_s = I_e (\Delta\rho)^2 VC (1 - C) \quad (3)$$

where C is volume fraction of the precipitates.

$$\tilde{Q}_s = \int_0^\infty sJ(s)\, ds = \int_0^{s_1} sJ(s)\, ds + \int_{s_1}^{s_2} sJ(s)\, ds + \int_{s_2}^\infty sJ(s)\, ds = \tilde{Q}_1 + \tilde{Q}_2 + \tilde{Q}_3 \quad (4)$$

where s_1 to s_2 is the range of s in which $J(s)$ can be obtained directly from experiments, 0 to s_1 is the range of s in which the scattering intensities can be obtained by extrapolation of the values of $J(s)$ in the range from s_1 to s_2, and s_2 to ∞ is the range in which Eq. [1] holds. Hence,

$$\tilde{Q}_3 = \int_{s_2}^\infty sJ(s)\, ds = K_p'/s_2 \quad (5)$$

The values of $\tilde{Q}_1$, $\tilde{Q}_2$, $\tilde{Q}_3$, and $\tilde{Q}_s$ obtained by Eqs. [4] and [5] are listed in Table I.

In Figure 4, $sJ(s) \sim s$ curves are shown; the area under the curve represents the value of $\tilde{Q}_2$.

It can be seen from Eq. [3] that $C(1 - C)$ is directly proportional to $\tilde{Q}_s$ if $(\Delta\rho)^2$, I_e, and V are constant. Thus, $\tilde{Q}_s$ changes with C. $C(1 - C)$ increases with the increase of C when $C < 0.5$; hence, the ratio of $\tilde{Q}_s$ shows a tendency of the change of the volume fraction. The ratio obtained from Table I is the following: $(\tilde{Q}_s)_1$; $(\tilde{Q}_s)_2$; $(\tilde{Q}_s)_3$; $(\tilde{Q}_s)_4$; $(\tilde{Q}_s)_5$; $(\tilde{Q}_s)_6$; $(\tilde{Q}_s)_7$ = 1:0. 92:1. 13:0. 94:1. 08:0. 90:1. 10, where subscript 1 is used for sample 1, 2 for sample 2, *etc.*

If we take $\tilde{Q}_s$ of the aged sample 1 as 1, then the $\tilde{Q}_s$ of sample 2 decreases to 0.92. It shows the tendency of decrease of C. The ratio increases to 1.13 for sample 3. It shows the tendency of increase of C.

It can be seen from Table I that the samples retrogressed at 200 °C for 90 seconds, 6 minutes, and 45-minutes have similar values of $\tilde{Q}_s$, and the samples retrogressed for various periods and then reaged have a different approximately constant value of $\tilde{Q}_s$ in the range of error of $\tilde{Q}_s$.

The gyration radius of the particle, R_G, is calculated from the $\ln J(h) \sim h^2$ plot[8,9] (Figure 5) in $h^2 > 0.2$ (nm^{-2}); here, $h = 2\pi s$ and $R_G^2 = \Sigma f_k R_k^2/n$; n is the total number of electrons in the particle, f_k is the scattering factor of the atom at point K in the particle, and R_k is the distance between point K and the electronic center of mass of the particle. The values of R_G are listed in Table I. A curvature occurs at the $\ln J(h) \sim h^2$ plot as $h^2 < 0.2$ (nm^{-2}). It shows the existence of some larger particles than those listed in Table I.

IV. DISCUSSION

Dahn *et al.* studied the changes of microstructure during retrogression and reaging in 7075 aluminum alloy by means of TEM. They showed that the drop in strength during ret-

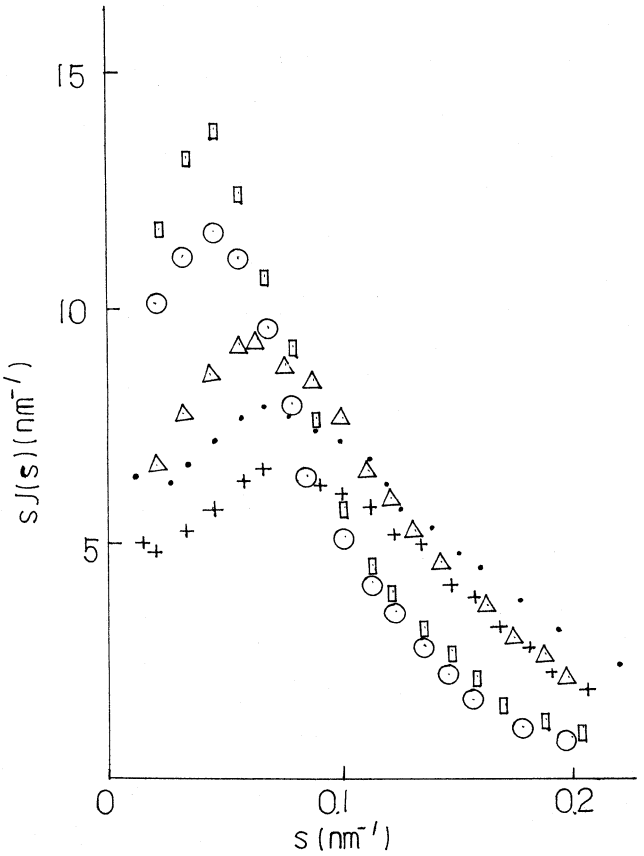

Fig. 4—*sJ* (*s*)-*s* plots: (·) for sample 1, (+) for sample 2, (△) for sample 3, (◯) for sample 4, and (□) for sample 5.

rogression was due to the partial dissolution of Guinier–Prestor (GP) zones, and reaging treatment resulted in the increase in volume fraction of the precipitates over both the T_6 and retrogressed conditions, thus, significantly improving the strength of the alloy.[2]

Although they believed that the high strength of the 7075 alloy in reaged sample arose from the relatively high overall concentration of the particles, no quantitative result was obtained.[2–6] The changes in hardness can be explained by the data of SAXS.

A. *The Changes in Hardness during Retrogression*

During retrogression at 200 °C, hardness initially decreases with an increase of retrogression time, achieves a minimum value at 90 seconds, increases, takes the second maximum value at 8 minutes, and finally decreases simply with further increasing retrogression time, as shown in Figure 1. The SAXS results show that at the beginning of retrogression, $\tilde{Q}_s$ decreases with the increase of retrogression time, there is a suggested decrease of C, and R_G increases. Partial dissolution of the particle occurs during retrogression, owing to the retrogression temperature being higher than aging temperature. The decrease of volume fraction of the precipitates and the growth of the particles result in the drop in hardness. The limit of solid solution is achieved at 200 °C for 90 seconds; hence, a minimum of hardness occurs. On the other hand, during retrogression, GP zone transforms partially to η' phase, and it leads to the increase in hardness.[2] Between the two effects discussed

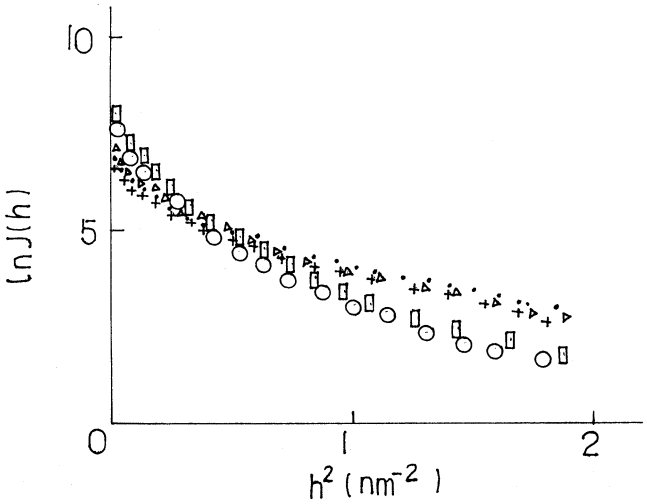

Fig. 5—Ln *J* (*h*)-h^2 plots: (·) for sample 1, (+) for sample 2, (△) for sample 3, (◯) for sample 4, and (□) for sample 5.

previously, the first effect is predominant until the minimum of hardness is achieved.

After the minimum of hardness is achieved, the second effect mentioned previously leads to an increase in hardness until the second maximum of hardness occurs. Finally, the $\tilde{Q}_s$ changes in the range of errors of $\tilde{Q}_s$, and the hardness drops simply with further increase of retrogression time, owing solely to coarsening of the precipitates.

B. *The Changes in Hardness during Reaging*

The hardness of the reaged sample is higher than that of the retrogressed sample. The hardness of the sample retrogressed at 200 °C for 6 minutes and then reaged takes the same value as that of the aged sample. The increase in hardness during reaging can be explained by SAXS results.

The value of $\tilde{Q}_s$ of the reaged sample is larger than those of the retrogressed and aged samples. During reaging, new precipitates occur, and they lead to the increase in hardness, whereas the hardness of the reaged samples, except the sample retrogressed at 200 °C for 6 minutes and then reaged, is still lower than that of the aged sample, owing to coarsening of the precipitates.

The error of $\tilde{Q}_s$ is from $\tilde{Q}_2$ and $\tilde{Q}_3$ mainly, because the value of s_1, $s_1 = 2 \sin (0.1 \text{ deg}/2)/\lambda$, is very small, and $\tilde{Q}_1$ contributes about 0.05 of the value of $\tilde{Q}_s$. The errors of $\tilde{Q}_1 + \tilde{Q}_2$ are about ± 0.02 (nm^{-2}). The error of $\tilde{Q}_3$ is from K_p' and is about ± 0.02 (nm^{-2}). The final error of $\tilde{Q}_s$ is about ± 0.04 (nm^{-2}), namely, it is about ± 0.02 of $\tilde{Q}_s$.

V. CONCLUSIONS

The following conclusions were drawn from the experimental results of SAXS.

1. The drop in hardness for short retrogression time is attributed to the decrease of volume fraction of the precipitates and the growth of the particle. The drop in hardness with increasing retrogression time after the second maximum of hardness is achieved is attributed to coarsening of the particles.
2. The increase in hardness during reaging is due to the

occurrence of new precipitates and the increase of volume fraction of the precipitates.

ACKNOWLEDGMENT

This project is supported by the State Key Laboratory for Corrosion and Protection, Academic Sinica.

REFERENCES

1. B. Cina: U.S. Patent No. 3,856,584, Dec. 24, 1974.
2. N.C. Danh, K. Rajan, and W. Wallace: *Metall. Trans. A*, 1983, vol. 14A, pp. 1843-50.
3. J.K. Park and A.J. Ardell: *Metall. Trans. A*, 1983, vol. 14A, pp. 1957-65.
4. J.K. Park and A.J. Ardell: *Metall. Trans. A*, 1984, vol. 15A, pp. 1531-43.
5. N. Danh, K. Rajan, and W. Wallace: *Metall. Trans. A*, 1985, vol. 16A, pp. 2068.
6. J.K. Park: *Mater. Sci. Eng.*, 1988, vol. A103, pp. 223-31.
7. C. Meng and Y. Wang: *Scripta Metall. Mater.*, 1990, vol. 24, pp. 1521-24.
8. A. Guinier and G. Fournet: *Small Angle Scattering of X-rays*, Wiley, New York, NY, 1955, pp. 17.
9. Chaofu Meng: *J. Non-Cryst. Solids*, 1991, vol. 130, pp. 107-09.
10. Chaofu Meng: *Sci. China*, 1994, vol. 37, pp. 870-77.